

RSC Advances



This is an *Accepted Manuscript*, which has been through the Royal Society of Chemistry peer review process and has been accepted for publication.

Accepted Manuscripts are published online shortly after acceptance, before technical editing, formatting and proof reading. Using this free service, authors can make their results available to the community, in citable form, before we publish the edited article. This *Accepted Manuscript* will be replaced by the edited, formatted and paginated article as soon as this is available.

You can find more information about *Accepted Manuscripts* in the [Information for Authors](#).

Please note that technical editing may introduce minor changes to the text and/or graphics, which may alter content. The journal's standard [Terms & Conditions](#) and the [Ethical guidelines](#) still apply. In no event shall the Royal Society of Chemistry be held responsible for any errors or omissions in this *Accepted Manuscript* or any consequences arising from the use of any information it contains.

1 **Electrochemical detection of cholesterol based on competitive host–guest**
2 **recognition using a β -cyclodextrin/poly(*N*-acetylaniline)/graphene-modified**
3 **electrode**

4

5 Long Yang^{a, 1}, Hui Zhao^{b, 1}, Shuangmei Fan^a, Genfu Zhao^a, Xin Ran^a, Can-Peng Li^{a,*}

6

7

8 ^a School of Chemical Science and Technology, Yunnan University, Kunming 650091,
9 PR China.

10 ^b Laboratory for Conservation and Utilization of Bio-resource, Yunnan University,
11 Kunming 650091, PR China.

12

13

14

15

16

17

18

19 ¹ These authors contributed equally to this work.

20 * Corresponding authors.

21 Fax or Tel: 86-871-65031119. E-mail: lcppp1974@sina.com (C.-P. Li);

22

23 **Abstract:** A sensitive and selective electrochemical approach for cholesterol sensing
24 based on a competitive host–guest recognition between β -cyclodextrin (β -CD) and
25 signal probe (Methylene blue)/target molecule (cholesterol) using
26 β -CD/poly(*N*-acetylaniline)/graphene (β -CD/PNAANI/Gra)-modified electrode was
27 developed. Due to the host–guest interaction, MB molecules can enter into the
28 hydrophobic inner cavity of β -CD, and the β -CD/PNAANI/Gra modified glassy
29 carbon electrode displays a remarkable anodic peak. In the presence of cholesterol,
30 competitive interaction to β -CD occurs and the MB molecules are displaced by
31 cholesterol. This results in a decreased oxidation peak current of MB. As MB is a well
32 known redox probe and hence can be easily detected using differential pulse
33 voltammetry technique. A linear response range of 1.00 to 50.00 μ M for cholesterol
34 with a low detection limit of 0.50 μ M ($S/N=3$) was obtained by using the indirectly
35 method. The proposed method could be successfully utilized to detect cholesterol in
36 serum samples, and may be expanded to analysis of other non-electroactive species.
37 Besides, the host–guest interaction between cholesterol and β -CD was studied by
38 molecular modeling calculations, which revealed that the complexation could reduce
39 the energy of the system and the complex of 2:1 host–guest stoichiometry had the
40 lowest ΔE value of -10.45 kcal/mol. The molecular docking studies suggested that
41 hydrogen bonding, electrostatic interactions, and hydrophobic interactions should be
42 the major driving forces for the formation of the inclusion complex.

43

44 **1. Introduction**

45 Cholesterol is a vital component in cells and tissues of humans, playing a
46 functional role in construction of cell membranes or serving as a biosynthetic
47 precursor of bile acids, vitamin D, steroid hormones etc. ¹ The normal level of total
48 cholesterol in healthy human serum is $\sim 200 \text{ mg dL}^{-1}$. ² Excess cholesterol in blood
49 serum forms plaques in the arteries of blood vessels which prevent the blood
50 circulation and cause cardiovascular diseases. ³ Thus the levels of total cholesterol in
51 serum and food are major parameters for diagnostic treatment. Over various analytical
52 methodologies, the electrochemical approach of different kinds of cholesterol
53 biosensing platforms has received great attention in past few decades as reviewed by
54 Arya et al. ⁴ Most of the cholesterol biosensors reported till date are based on the
55 detection of electrooxidation of hydrogen peroxide produced during the catalysis of
56 cholesterol by cholesterol oxidase. ⁵ This requires a high anodic potential that can
57 induce simultaneous oxidation of other electrochemically active species present in
58 samples leading to false positive signals. Besides, detection selectivity in these
59 methods relies on the use of cholesterol selective enzymes which are expensive,
60 unstable, and prone to denaturation. ³ Therefore, an alternative, simple, and cost
61 effective method for the sensitive and selective detection of cholesterol is highly
62 desirable.

63 The concept of indicator displacement assay (IDA) has received considerable
64 interest with the development of supramolecular chemistry, which exploit the
65 potential of artificial receptors, particularly macrocyclic hosts, for its promising
66 applications in molecular recognition and sensing. ^{6,7} The sensing principle of IDA

67 relies on the competition between a test substance and an indicator for the same
68 binding site on the host.⁸ When an analyte is added to a solution containing
69 host-indicator complex, the analyte displaces the indicator from the binding site.
70 Upon displacement of the indicator, a change in signal is observed. Cyclodextrins
71 (CDs) as the typical macrocyclic molecules have toroidal shapes with hydrophobic
72 inner cavities and hydrophilic exteriors.⁹ The interesting characteristics can enable
73 them to bind a wide variety of hydrophobic guest molecules to form stable host-guest
74 complex in their hydrophobic cavity.¹⁰ The host-guest interaction between β -CD and
75 cholesterol has been used for cholesterol extraction from bioenvironment such as food,
76 cell membranes, blood serum and cultured cells.³ This suggests that β -CD can be an
77 alternative to cholesterol enzyme for selective recognition of cholesterol. However,
78 this interaction does not produce any signal change. In addition, cholesterol is one of
79 the non-electroactive species, resulting its direct electrochemical determination is very
80 difficult. Alternatively, designing a competitive host-guest recognition system by
81 selecting an electroactive probe as signal indicator might have promising applications
82 for the analysis of non-electroactive species. Mondal and Jana³ have recently carried
83 out fluorescent detection of cholesterol using graphene - β -CD (Gra- β -CD) hybrid
84 system, where the optical detection of cholesterol was carried out using rhodamin 6G
85 (R6G) dye as a fluorophore. Although the competitive host-guest interaction system
86 has been widely applied in the fluorescent sensing filed,^{3,11-15} it is rarely investigated
87 for electrochemical sensing applications except few researchers contributed to this
88 area.^{16,17}

89 Herein, a non-enzymatic electrochemical approach for cholesterol sensing based
90 on a competitive host-guest recognition between β -CD and signal probe/target
91 molecules using β -CD/poly(*N*-acetylaniline)/Gra (β -CD/PNAANI/Gra)-modified
92 electrode was proposed. Methylene blue (MB) and cholesterol were selected as the
93 probe and target molecules, respectively. Gra was chosen here considering that it can
94 enhance the electrode conductivity and facilitate the electron transfer. The
95 introduction of PNAANI film is used to steadily immobilize β -CD and to avoid the
96 non-specific adsorption of MB on the Gra film by a π - π stacking interaction. Due to
97 the host-guest interaction, MB molecules can enter into the hydrophobic inner cavity
98 of β -CD, and the β -CD/PNAANI/Gra modified glassy carbon electrode displays a
99 remarkable anodic peak. In the presence of cholesterol, competitive interaction to
100 β -CD occurs and the MB molecules are displaced by cholesterol. This results in a
101 decreased oxidation peak current of MB. As MB is a well known redox probe and
102 hence can be easily detected using differential pulse voltammetry (DPV) technique.
103 Agnihotri et al.¹⁷ reported an electrochemical detection of cholesterol using
104 Gra- β -CD hybrid as the sensing matrix, while the host-guest interaction in their work
105 did not occur on the electrode surface (in an electrochemical cell). Compared with this
106 previous report, the host-guest interaction in the present work occurred completely on
107 the β -CD/PNAANI/Gra-modified electrode surface, which is less expensive as an
108 electrochemical cell needs 3 mL materials. And the non-specific adsorption of MB on
109 the Gra film was avoided by the PNAANI film. The proposed method could be
110 successfully utilized to detect cholesterol in serum samples, and exhibited a promising

111 application in practice. In addition, the host–guest interaction between cholesterol and
112 β -CD was investigated by molecular modeling calculations.

113

114 **2. Materials and methods**

115 **2.1. Chemicals**

116 Graphite oxide was purchased from Nanjing XFNANO Materials Tech Co., Ltd.
117 (Nanjing, China). Cholesterol, MB, β -CD, and *N*-acetylaniline (NAANI) were
118 obtained from Sigma Chemical Co. (St. Louis, MO, USA). All other reagents were of
119 analytical grade. Phosphate buffer (PBS, 0.1 M pH 7.0) was used as working solution.
120 All aqueous solutions were prepared with deionized water (DW, 18 M Ω cm).

121

122 **2.2. Apparatus**

123 Electrochemical impedance spectroscopy (EIS) and DPV experiments were
124 performed with a CHI 660E Electrochemical Workstation from Shanghai Chenhua
125 Instrument (Shanghai, China) and conducted using a three-electrode system, with the
126 modified GCE as working electrode, a platinum wire as the counter electrode, a
127 saturated calomel electrode (SCE) as the reference electrode. The morphologies of the
128 prepared samples were characterized by a QUNT200 scanning electron microscopy
129 (SEM, USA). UV–visible spectra were analyzed in a U-2001 Hitachi (Tokyo, Japan)
130 UV spectrophotometer. Fourier transform infrared (FTIR) study was performed over
131 the wavenumber, range of 4000–400 cm⁻¹ by a Thermo Fisher SCIENTIFIC Nicolet
132 IS10 (Thermo Fisher, Massachusetts, USA) FTIR impact 410 spectrophotometer

133 using KBr pellets. Raman spectra were obtained on a 400F PERKINELMER Raman
134 spectrometer (USA) with 514.5 nm wavelength incident laser light.

135

136 **2.3. Molecular docking**

137 The crystal structures of β -CD (ID: IHEGEI) and cholesterol (ID: CHOEST21)
138 were obtained from Cambridge Crystallographic Data Centre (CCDC) and optimized
139 using molecular dynamics simulation with the Gaussian 03 program. Both the
140 optimized structures were used as a starting structure in the docking study.
141 AutoDock4.2 with Lamarckian Genetic Algorithm (LGA) was used for docking study.
142 An initial population of 150 individuals with a maximum number of energy
143 evaluations of 25,000,000 and a maximal number of generations of 27,000 were used
144 as an end criterion. An elitism value of one was used and a probability of mutation
145 and crossing-over of 0.02 and 0.8 was used, respectively. We have defined the
146 conformational search space implementing an $60 \times 60 \times 60$ grid and 0.375 Å spacing
147 between each point in such a way that it covered both the external surface and the
148 internal cavity of the β -CD. A total of 50 docking runs were carried out. At the end of
149 each run, the solutions were separated into clusters according to their lowest RMSD
150 and the best energy score value based on an empirical free energy function. Clustering
151 was performed on the docked complexes with a cut-off of 2 Å. From the docking
152 calculations, the lowest energy conformation was selected as the cholesterol/ β -CD
153 binding mode, and the binding free energy of the cholesterol/ β -CD complex was
154 calculated by using the semi-empirical method PM3.

155

156 2.4. Preparation of the Gra

157 The graphite oxide was exfoliated into graphene oxide (GO) sheets by
158 ultrasonication at room temperature for one hour. The as-obtained yellow-brown
159 aqueous suspension of GO was stored at room temperature and used for further
160 experiment. Compared with the traditional procedure using highly toxic hydrazine as
161 reductant, ascorbic acid (AA) was used as reducing agent to prepare Gra in DW at
162 room temperature. In a typical experiment, 50 mg of AA was added into 10.0 mL of
163 0.5 mg mL⁻¹ GO aqueous suspension and stirred for 48 h at room temperature. After
164 centrifuging and washing with DW for three times, the resulting Gra material was
165 obtained by freeze-drying.

166

167 2.5. Preparation of the modified electrodes

168 Glassy carbon electrode (GCE, 3 mm in diameter) was polished with 0.3 and 0.05
169 μm Al₂O₃ powder respectively and subsequently sonicated in ethanol and DW to
170 remove the adsorbed substance and dried in air. The Gra was dissolved in DW at a
171 concentration of 0.5 mg mL⁻¹ with the aid of ultrasonic agitation for 20 min, resulting
172 in a homogeneous suspension. To prepare the Gra modified electrode, 5 μL of the Gra
173 suspension was dropped onto the electrode surface and dried at room temperature.
174 The obtained electrode was noted as Gra/GCE. In order to prepare the
175 PNAANI/Gra/GCE, the Gra/GCE was held at a constant voltage of 1.0 V for 1 min in
176 a mixture solution containing 0.1 M NAANI and 1.0 M HClO₄ aqueous solution, and

177 then swept from -0.2 to 1.0 V for 25 cycles at a scan rate of 100 mV s^{-1} . Finally, by
178 electro-oxidation of the PNAANI/Gra/GCE at a constant potential of 1.2 V for 12 min
179 by amperometric $i-t$ curve technique in a mixture solution containing 0.05 M β -CD
180 and 0.1 M LiClO_4 in DMSO, the β -CD/PNAANI/Gra/GCE was obtained successfully.
181 For comparison, a similar procedure was used to prepare PNAANI/Gra/GCE
182 and β -CD/PNAANI/GCE.

183

184 **2.6. Electrochemical measurements**

185 DPV was applied in 0.1 M pH 7.0 PBS from -0.7 to 0.7 V with a pulse amplitude
186 of 0.05 V and a pulse width of 0.05 s. EIS was recorded in the frequency range from
187 10^{-1} to 10^5 Hz with an amplitude of 5 mV using 2.0 mM $[\text{Fe}(\text{CN})_6]^{3-/4-}$ redox couple
188 (1:1) with 0.1 M KCl as supporting electrolyte. All the measurements were carried out
189 at room temperature. As cholesterol has very low solubility in water, 1.0 mM stock
190 solution of cholesterol was prepared in ethanol and diluted to different concentrations
191 by 0.1 M pH 7.0 PBS for further use. Before electrochemical measurements, the
192 β -CD/PNAANI/Gra/GCE was incubated with 1.0 mM MB solution (in 0.1 M pH 7.0
193 PBS) for a definite time, and rinsed gently with ultrapure water. Then, the electrode
194 was further incubated with different concentrations of cholesterol solution. After that,
195 the electrode was rinsed gently with ultrapure water and the current response of the
196 MB-bound β -CD/PNAANI/Gra/GCE were investigated by DPV in 0.1 M pH 7.0
197 PBS.

198

199 3. Results and Discussion

200 3.1. Design strategy of the electrochemical sensor

201 **Scheme 1** illustrates the assay protocol of the proposed electrochemical sensor
202 based on the competitive host–guest interaction between β -CD and MB (signal
203 probe)/cholesterol (target). MB molecules can enter into the inner cavity of β -CD due
204 to the host–guest interaction, and the MB-bound β -CD/PNAANI/Gra/GCE displays a
205 remarkable oxidation peak due to MB. However, in the presence of cholesterol,
206 competitive association to the β -CD occurs and the MB molecules are displaced by
207 cholesterol. This results in a decrease of the oxidation peak current of the MB probe.

208

209 3.2. Molecular docking

210 In recent years, widespread use has been made of computer aided molecular
211 modeling to rapidly and simply obtain a three dimensional image of the most likely
212 structure of the inclusion complex. Typically, the more negative the binding energy is,
213 the stronger interaction is between the host and guest molecules. As listed in **Table 1**,
214 the lowest binding free energy (ΔE) was -6.68 kcal/mol for the host–guest complex
215 of cholesterol and β -CD with 1:1 stoichiometry calculated by PM3 method. The
216 lowest energy docked conformation for 1:1 complex of cholesterol and β -CD, shown
217 in **Fig. 1A**, reveals that the B-, C-, and D-rings of cholesterol molecule inserted into
218 β -CD cavity due to hydrophobic interactions, however, the cyclohexanol part (A-ring)
219 and the alkyl chain of the cholesterol molecule located just outside the β -CD host. The
220 A-, B-, C-, and D-rings of cholesterol were indicated in **Scheme 2**. Among all the

221 docking conformations of cholesterol and β -CD, two other conformations capture our
222 attention. One is the cyclohexanol part (A-ring) that inserted into the cavity of β -CD,
223 the other is the alkyl chain of the cholesterol that inserted into β -CD cavity. Thus, we
224 speculated that one cholesterol molecule may bind with two β -CD molecules to form
225 a 1:2 inclusion complex. So we have further studied the interaction between one
226 cholesterol and two β -CD molecules. The crystal structure of two adjacent β -CDs (ID:
227 WISRIZ) was obtained from Cambridge Crystallographic Data Centre (CCDC) and
228 also optimized using molecular dynamics simulation with the Gaussian 03 program.
229 The docked conformation was displayed in **Fig. 1B**, indicating that the cyclohexanol
230 (A-ring) and the alkyl chain of cholesterol molecule inserted into the cavities of two
231 β -CD molecules, respectively. The ΔE calculated by PM3 method was -10.45
232 kcal/mol, which is much lower than that of a 1:1 inclusion complex, indicating
233 that a 1:2 guest–host binding mode is more stable. Analysis of host–guest interaction
234 as obtained from the docking studies reveals that hydrogen bonding, electrostatic
235 interactions, and hydrophobic interactions are the predominant driving forces of the
236 1:2 guest–host complex. Firstly, the hydroxyl on A-ring of the cholesterol molecule
237 formed hydrogen bonding with the hydroxyl of β -CD and the bond length is 2.0 \AA .
238 Secondly, as shown in **Fig. 1C**, the surface of cholesterol molecule is mainly
239 negatively charged, while the internal cavities of the two adjacent β -CDs are mainly
240 positively charged. Thus, strong electrostatic interactions formed between cholesterol
241 molecule and the two β -CDs. Thirdly, as revealed in **Fig. 1D**, strong hydrophobic
242 interactions also formed between cholesterol molecule and the two β -CDs. The

243 cyclohexanol and the alkyl chain groups of the cholesterol molecule inserted into the
244 hydrophobic cavities of two β -CD molecules, respectively. Recently, Cheng et al.¹⁸
245 proposed a similar 1:2 cholesterol/ β -CD complex structure based on the 2D ^1H
246 ROESY results. This result is in accordance with that of our obtained from molecular
247 docking.

248

249 **3.3. Characterization of the β -CD/PNAANI/Gra/GCE film**

250 The reduction of the GO was characterized by UV–visible spectroscopy, FTIR
251 spectroscopy, and Raman spectroscopy, respectively. Initially, UV–visible
252 spectroscopy was used to study the reduction of GO. As shown in **Fig. 2A**, the GO
253 shows a strong absorption at 230 nm and a shoulder at 300 nm, which correspond to
254 the π – π^* transition of the aromatic C=C bond and the n– π^* transition of the C=O
255 bond, respectively. After reduction, the peak at 230 nm shifts to 260 nm indicating the
256 restoration of the π -conjugation network of the Gra. The disappearance of the peak at
257 300 nm reflects the effect of deoxygenation. To further illustrate the formation of Gra,
258 FTIR spectra were employed to investigate the reduction of GO. **Fig. 2B** shows the
259 FTIR spectra of the GO and Gra. As observed, the GO displays several characteristic
260 bands at approximately 3425, 1724, 1617, 1213, and 1052 cm^{-1} , which are caused by
261 the stretching vibrations of –OH, C=O, C=C, C–O–C, and C–O, respectively. After
262 reduction, the band at 1724 cm^{-1} corresponding to the C=O stretch vanishes, and the
263 bands at 3425 and 1213 cm^{-1} decreases dramatically, confirming that the GO was
264 reduced to Gra by AA. Raman spectroscopy is one of the most widely used techniques

265 to characterize the structural and electronic properties of Gra including disordered and
266 defective structures, defect density, and doping levels. **Fig. 2C** shows the typical
267 Raman spectra of GO and Gra. As expected, GO displays two prominent peaks at
268 1360 and 1602 cm^{-1} corresponding to the D and G bands, respectively. The Gra shows
269 two prominent peaks at 1355 and 1589 cm^{-1} , corresponding to the breathing mode of
270 k-point phonons of A_{1g} symmetry (D band) and the E_{2g} phonons of C sp^2 atoms (G
271 band) of Gra, respectively. The intensity ratio of the D band to the G band (I_D/I_G) is
272 clearly higher when compared with that of GO (0.97 vs. 0.78), suggesting a decrease
273 in sp^2 domains and a partially ordered crystal structure of Gra induced by AA
274 reduction.

275 Because the PNAANI and β -CD were immobilized on the Gra/GCE by
276 electro-polymerization electro-oxidation, respectively. It is difficult to characterize by
277 FTIR. Thus, the Gra/GCE, PNAANI/Gra/GCE, and β -CD/PNAANI/Gra/GCE films
278 were investigated using SEM. As shown in **Fig. 3A**, the microstructure image reveals
279 that after reduction the Gra material consists of randomly aggregated thin, wrinkled
280 sheets closely associated with each other. It is noted that after polymerization of
281 NAANI on the surface of Gra/GCE, a layer of PNAANI was densely covered on the
282 surface of Gra/GCE (**Fig. 3B**). Besides, it can be seen from **Fig. 3C** that a layer of
283 β -CD thin films was uniformly covered on the surface of PNAANI/Gra/GCE,
284 indicating that the β -CD/PNAANI/Gra/GCE film was successfully obtained.

285

286 **3.4. Electrochemical characterization of the modified electrodes**

287 EIS was performed at the potential of 0.1 V and the frequency ranges was from
288 10^1 to 10^5 Hz, using 2.0 mM $[\text{Fe}(\text{CN})_6]^{3-/4-}$ redox couple (1:1) with 0.1 M KCl as
289 supporting electrolyte. The value of the electron-transfer resistance (R_{ct}) of the
290 modified electrode was estimated by the semicircle diameter. **Fig. 4A** illustrates the
291 EIS of the bare GCE, Gra/GCE, β -CD/PNAANI/GCE, and β -CD/PNAANI/Gra/GCE.
292 Obviously, the bare GCE exhibited a semicircle portion and the value of R_{ct} was
293 estimated to be 750 Ω . While the R_{ct} decreased remarkably at Gra/GCE, indicating
294 that Gra had good conductivity and improved obviously the diffusion of ferricyanide
295 toward the electrode interface. In the case of β -CD/PNAANI/GCE, its R_{ct} further
296 increased to 1500 Ω due to the poor conductivity of β -CD, suggesting that large
297 amount of β -CD molecules were successfully immobilized on the surface of
298 PNAANI/GCE. Furthermore, the R_{ct} of the β -CD/PNAANI/GCE is much larger than
299 that of the β -CD/PNAANI/Gra/GCE, although the introduction of β -CD results in the
300 increase of the semicircle diameter. These results indicate that the Gra film can
301 significantly accelerate the interfacial charge transfer between the electrochemical
302 probe $[\text{Fe}(\text{CN})_6]^{3-/4-}$ and the modified electrode, which will be beneficial to the good
303 analytical performance of the electrode.

304 **Fig. 4B** shows the DPV responses of different electrodes in 0.1M pH 7.0 PBS
305 after incubation with 1.0 mM MB. On the Gra/GCE (**curve a**), an oxidation peak was
306 observed due to the non-specific adsorption of MB on Gra via π - π stacking. However,
307 there is no oxidation peak of MB on the PNAANI/Gra/GCE (**curve b**), indicating that
308 the adsorption of MB was restrained by PNAANI film. Furthermore, on the

309 β -CD/PNAANI/Gra/GCE (**curve d**), the oxidation peak current of MB increases
310 obviously due to the good molecular recognition property and high enrichment
311 capability of β -CD compared to all the other electrodes. As a comparison, the DPV
312 response of MB on the β -CD/PNAANI/GCE was also investigated (**curve c**). It is
313 noted that the peak current is smaller than that on the β -CD/PNAANI/Gra/GCE.
314 These imply that the large specific surface area and good electron transfer property of
315 Gra are important to improve the electrochemical performance of the modified
316 electrode. In general, it can be concluded that the introduction of Gra film is
317 beneficial to enhancing the electron transfer of the electrochemical sensor, and the
318 PNAANI film can avoid successfully the non-specific adsorption of MB on Gra film
319 via π - π stacking interaction.

320

321 **3.5. Feasibility of the electrochemical sensor**

322 To demonstrate the assay feasibility of the proposed sensor, DPV response of the
323 β -CD/PNAANI/Gra/GCE was investigated in 0.1 M pH 7.0 PBS. As can be seen from
324 **Fig. 4C**, no detectable signal (**curve a**) is observed for the β -CD/PNAANI/Gra/GCE
325 in 0.1 M pH 7.0 PBS due to the absence of the redox mediator MB. After incubated in
326 1.0 mM MB solution for 25 min, the MB-bound β -CD/PNAANI/Gra/GCE was then
327 tested in 0.1 M pH 7.0 PBS and an obvious oxidation peak of MB (**curve b**) can be
328 observed at about -0.1 V. When the β -CD/PNAANI/Gra/GCE was first incubated in
329 1.0 mM MB solution for 25 min and further incubated in 10 μ M cholesterol solution
330 for 30 min, then tested in 0.1 M pH 7.0 PBS, a decreased oxidation peak (**curve c**)

331 was obtained due to competitive association of cholesterol/MB to the β -CD occurs.
332 This is because cholesterol has higher binding affinity to β -CD cavity due to its
333 hydrophobic nature. This suggests that the MB molecules present inside the
334 β -CD/PNAANI/Gra/GCE host can be replaced by cholesterol and the MB-bound
335 β -CD/PNAANI/Gra/GCE can be used to sensitively detect cholesterol by the
336 competitive electrochemical sensing strategy.

337

338 **3.6. Optimization of experimental conditions**

339 Several control experiments were carried out to determine the optimum reaction
340 conditions. **Fig. 5A** shows the effect of the potential cycle number of the
341 electrodeposition of PNAANI film on the DPV peak current of the
342 PNAANI/Gra/GCE in 0.1 M pH 7.0 PBS after incubation in 1.0 mM MB solution. It
343 is noted that the oxidation peak current of MB decreases with an increase of the cycle
344 number and reaches about 0 at 25 cycles, indicating that the surface of Gra/GCE is
345 covered completely by PNAANI film and that the PNAANI/Gra/GCE can
346 successfully avoid the non-specific adsorption of MB on the surface of Gra by π - π
347 stacking interactions. Therefore, a cycle number of 25 was selected for further study.
348 Moreover, the effect of the electro-oxidation time of β -CD on the DPV peak current
349 of the β -CD/PNAANI/Gra/GCE was also investigated (**Fig. 5B**). Due to the
350 host-guest interaction between MB and β -CD, it was found that the peak current of
351 MB increases with the increase of the deposition time and a maximum is observed at
352 12 min. This suggests that the immobilized amount of β -CD is at a maximum at 12

353 min. Thus, this time was selected as the optimum electro-oxidation time for β -CD on
354 the PNAANI/Gra/GCE. In addition, the incubation time of the modified electrode in
355 MB solution is one of the key parameters that will affect the response performance of
356 the electrode. **Fig. 5C** shows that the oxidation peak current of the electrode increases
357 with the increase of the incubation time and reaches a maximum at 25 min for MB
358 incubation. Therefore, 25 min is selected as the optimum incubation time for the
359 as-prepared electrode in MB solution. Similarly, the effect of the incubation time of
360 the modified electrode in cholesterol solution was also studied. **Fig. 5D** shows that the
361 oxidation peak current of the electrode decreases with the increase of the incubation
362 time and reaches about 0 at 30 min for cholesterol incubation. Therefore, 30 min is
363 selected as the optimum incubation time for the as-prepared electrode in cholesterol
364 solution.

365

366 **3.7. Quantitative analysis of the electrochemical sensor toward cholesterol**

367 Under optimal conditions, DPV was used to determine the concentrations of
368 cholesterol because it is a highly sensitive and low-detection limit electrochemical
369 method. **Fig. 6A** shows the DPV curves of electrochemical signal on the MB-bound
370 β -CD/PNAANI/Gra/GCE under different concentrations of cholesterol solution. The
371 oxidation peak currents of MB decreased with increased cholesterol concentrations.
372 **Fig. 6B** shows the corresponding calibration curve for cholesterol quantification. The
373 peak currents were proportional to the cholesterol concentrations between 1.00 and
374 50.00 μ M with a detection limit of 0.50 μ M ($S/N=3$). The corresponding regression

375 equation was calculated as $\Delta I (\mu A) = 0.154C (\mu M) + 0.588$ with correlation
376 coefficients of 0.998. Detection limit was less than 1.0 μM which was quite low and
377 satisfactory with respect to other recently reported articles. **Table 2** illustrates few of
378 the recent literatures on cholesterol sensing platforms, through both enzymatic and
379 non-enzymatic sensing routes. The detection limit and sensitivity of the present
380 sensing strategy is comparatively better than the reported ones.

381

382 **3.8. Selectivity, reproducibility, and stability**

383 As we know, human blood serum contains many more biocomponents like salts,
384 amino acids, carbohydrates, lipids etc., those can interfere with cholesterol detection
385 and hamper the selectivity of the electrochemical sensor. Therefore, we have tested
386 interference from common molecules present in human blood serum and found very
387 negligible interference. As shown in **Fig. 6C**, some salts, carbohydrates, protein,
388 anionic surfactant, etc. including glucose, AA, bovine serum albumin (BSA), sodium
389 dodecyl sulphate (SDS), NaCl, KCl, and, $MgCl_2$ showed negligible interference even
390 at the concentration of 2.0 mM, compared to cholesterol detected for only 30 μM
391 concentration. Six equal MB-bound β -CD/PNAANI/Gra/GCEs were used to evaluate
392 the fabrication reproducibility of the present method for cholesterol detection. The six
393 modified electrodes exhibited similar signals with a relative standard deviation of
394 3.9%, indicating satisfactory reproducibility. Additionally, a long-term stability
395 experiment was performed intermittently (every 5 days) and used to examine the
396 stability of the MB-bound β -CD/PNAANI/Gra/GCE. The constructed sensor was

397 stored in a refrigerator at 4 °C when not in use. Initial responses of over 94.3% and
398 85.6% remained after storage for 15 and 30 days, respectively, indicating an
399 acceptable stability of the MB-bound β -CD/PNAANI/Gra/GCE.

400

401 **3.9. Real sample analysis**

402 The proposed method was used to detect cholesterol in serum samples using
403 standard addition methods to evaluate the feasibility of the MB-bound
404 β -CD/PNAANI/Gra/GCE for real sample analysis. The serum sample was diluted
405 fifty times with 0.1 M pH 7.0 PBS. Results showed recoveries ranging from 98.4% to
406 105.2% and RSDs ranging from 2.6% to 4.5% (**Table 3**). The results demonstrated
407 that this method can be extended for cholesterol detection in blood.

408 The proposed sensing platform may also be expanded to wide and potential
409 applications in biological and environmental samples. It is worthy note that, as an
410 oligosaccharide, β -CD is more stable than cholesterol selective enzymes (mostly
411 oxidase) under complex conditions. Thus the present sensing platform seems to be
412 more suitable for analysis of practical cholesterol samples than traditional
413 enzyme-based biosensor.

414

415 **4. Conclusions**

416 In conclusion, based on a competitive host-guest interaction between β -CD and
417 signal probe/target molecules, a new electrochemical approach for cholesterol sensing
418 using β -CD/PNAANI/Gra-modified electrode was developed. Due to the good

419 electron transfer property of the Gra, the excellent inhibiting ability of PNAANI film
420 for the non-specific adsorption of MB, and the excellent host–guest recognition of
421 β -CD, the developed β -CD/PNAANI/Gra/GCE displays excellent analytical
422 performance for the electrochemical detection of cholesterol: the linear response
423 range is 1.00–50.00 μ M and the LOD is 0.50 μ M ($S/N=3$). In addition, the developed
424 electrochemical sensing platform is important as it does not use any enzyme or
425 antibody for detection of cholesterol efficiently with outstanding selectivity over the
426 common interfering species. Besides, the host–guest interaction between cholesterol
427 and β -CD was studied by molecular modeling calculations, which revealed that the
428 complexation could reduce the energy of the system and the complex of 2:1
429 host–guest stoichiometry had the lowest ΔE value of -10.45 kcal/mol. The molecular
430 docking studies suggested that hydrogen bonding, electrostatic interactions, and
431 hydrophobic interactions should be the predominant driving forces for the formation
432 of the inclusion complex.

433

434 **Acknowledgements**

435 This work was supported by the Natural Science Foundation of China (31160334)
436 and the Natural Science Foundation of Yunnan Province (2012FB112, 2014RA022),
437 People's Republic of China.

438

439 **References:**

440 1 N. Batra, M. Tomar, V. Gupta, *Biosens. Bioelectron.*, 2015, **67**, 263–271.

- 441 2 J. Motonaka, L. R. Faulkner, *Anal. Chem.*, 1993, **65**, 3258–3261.
- 442 3 A. Mondal, N. R. Jana, *Chem. Commun.*, 2012, **48**, 7316–7318.
- 443 4 S. K. Arya, M. Datta, B. D. Malhotra, *Biosens. Bioelectron.*, 2008, **23**,
444 1083–1100.
- 445 5 U. Saxena, M. Chakraborty, P. Goswami, *Biosens. Bioelectron.*, 2011, **26**,
446 3037–3043.
- 447 6 F. Biedermann, V. D. Uzunova, O. A. Scherman, W. M. Nau, A. D. Simone, *J.*
448 *Am. Chem. Soc.*, 2012, **134**, 15318–15323.
- 449 7 F. Biedermann, M. Vendruscolo, O. A. Scherman, A. D. Simone, W. M. Nau, *J.*
450 *Am. Chem. Soc.*, 2013, **135**, 14879–14888.
- 451 8 G. Ghale, W. M. Nau, *Acc. Chem. Res.*, 2014, **47**, 2150–2159.
- 452 9 Y. Guo, S. Guo, J. Ren, Y. Zhai, S. Dong, E. Wang, *ACS Nano*, 2010, **4**,
453 4001–4010.
- 454 10 G. B. Zhu, X. Zhang, P. B. Gai, X. H. Zhang, J. H. Chen, *Nanoscale*, 2012, **4**,
455 5703–5709.
- 456 11 F. Biedermann, W. M. Nau, *Angew. Chem. Int. Ed.*, 2014, **53**, 5694–5699.
- 457 12 C. Li, J. Feng, H. X. Ju, *Analyst*, 2015, **140**, 230–235.
- 458 13 G. Ghale, V. Ramalingam, A. R. Urbach, W. M. Nau, *J. Am. Chem. Soc.*, 2011,
459 **133**, 7528–7535.
- 460 14 J. M. Chinai, A. B. Taylor, L. M. Ryno, N. D. Hargreaves, C. A. Morris, P. John
461 Hart, A. R. Urbach, *J. Am. Chem. Soc.*, 2011, **133**, 8810–8813.
- 462 15 X. Mao, D. Tian, H. Li, *Chem. Commun.*, 2012, **48**, 4851–4853.

- 463 16 G. B. Zhu, L. Wu, X. Zhang, W. Liu, X. H. Zhang, J. H. Chen, *Chem. Eur. J.*,
464 2013, **19**, 6368 – 6373.
- 465 17 N. Agnihotri, A. D. Chowdhury, A. De, *Biosens. Bioelectron.*, 2015, **63**,
466 212–217.
- 467 18 Y. Cheng, P. Jiang, S. Lin, Y. Li, X. Dong, *Sens. Actuators B*, 2014, **193**,
468 838–843.
- 469 19 L. Zhu, L. Xu, L. Tan, H. Tan, S. Yang, S. Yao, *Talanta*, 2013, **106**, 192–199.
- 470 20 C. Z. Zhao, L. Wan, L. Jiang, Q. Wang, K. Jiao, *Anal. Biochem.*, 2008, **383**,
471 25–30.
- 472 21 N. Ruecha, R. Rangkupan, N. Rodthongkum, O. Chailapakul, *Biosens.*
473 *Bioelectron.*, 2014, **52**, 13–19.
- 474 22 A. Ahmadalinezhad, A. C. Chen, *Biosens. Bioelectron.*, 2011, **26**, 4508–4513.
- 475 23 A. K. Giri, A. Sinhamahapatra, S. Prakash, J. Chaudhari, V. K. Shahi, A. B.
476 Panda, *J. Mater. Chem. A*, 2013, **1**, 814–822.
- 477 24 A. Umar, R. Ahmad, S. W. Hwang, S. H. Kim, A. Al-Hajry, Y. B. Hahn,
478 *Electrochim. Acta*, 2014, **135**, 396–403.

479

480 **Figure captions:**

481

482 **Scheme 1.** Illustration of the strategy of the proposed electrochemical sensor based on
483 the competitive host–guest interaction between β -CD and MB (signal
484 probe)/cholesterol (target).

485

486 **Scheme 2.** The chemical structure of cholesterol.

487

488 **Fig. 1.** Lowest energy cholesterol/ β -CD docked complex for 1:1 (**A**) and 2:1 (**B**)

489 host–guest stoichiometry (left is the side view, right is the top view). The electrostatic

490 forces (**C**, left is the bottom view, right is the top view; red represents the strongest

491 positively charged, blue represents the strongest negatively charged) and hydrophobic

492 forces (**D**, left is the side view, right is the bottom view; brown represents the493 strongest hydrophobic, blue represents the strongest hydrophilic) of cholesterol/ β -CD

494 docked complex for 2:1 host–guest stoichiometry.

495

496 **Fig. 2.** UV–vis absorption spectra (**A**), FTIR spectra (**B**), and Raman spectra (**C**) of

497 GO and Gra.

498

499 **Fig. 3.** SEM images of Gra/GCE (**A**), PNAANI/Gra/GCE (**B**), and500 β -CD/PNAANI/Gra/GCE (**C**).

501

502 **Fig. 4.** (**A**) EIS characterization of GCE, Gra/GCE, β -CD/PNAANI/GCE, and503 β -CD/PNAANI/Gra/GCE. using 2.0 mM $[\text{Fe}(\text{CN})_6]^{3-/4-}$ redox couple (1:1) with 0.1 M504 KCl as supporting electrolyte. (**B**) DPV responses of the Gra/GCE (a),505 PNAANI/Gra/GCE (b), β -CD/PNAANI/GCE (c), and β -CD/PNAANI/Gra/GCE (d)506 in 0.1M pH 7.0 PBS after incubation with 1.0 mM MB. (**C**) DPV response of the

507 β -CD/PNAANI/Gra/GCE in 0.1 M pH 7.0 PBS **(a)**, incubated in 1.0 mM MB solution
508 for 25 min **(b)**, and further incubated in 10 μ M cholesterol solution for 30 min then
509 tested in 0.1 M pH 7.0 PBS **(c)**.

510

511 **Fig. 5.** Effects of the cycle number of the CV deposition of PNAANI **(A)** and the
512 electro-oxidation time of β -CD **(B)** on the DPV peak currents of the
513 PNAANI/Gra/GCE in 0.1 M pH 7.0 PBS after incubation in 1.0 mM MB solution.
514 Effects of incubation time on the DPV peak currents of the β -CD/PNAANI/Gra/GCE
515 in 0.1 M pH 7.0 PBS after incubation in 1.0 mM MB solution **(C)** and further
516 incubated in 50 μ M cholesterol solution **(D)**.

517

518 **Fig. 6.** **(A)** DPV curves of the proposed sensing platform under different
519 concentrations of cholesterol. **(B)** Calibration curves for the determination of
520 cholesterol using the proposed sensor. The error bars represent the standard deviations
521 of three parallel tests. **(C)** Interference studies using different species in the developed
522 cholesterol detection method, using DPV and keeping all the parameters constant. The
523 cholesterol concentration is 30 μ M against the concentration of all other substances,
524 which is kept at 2.0 mM.

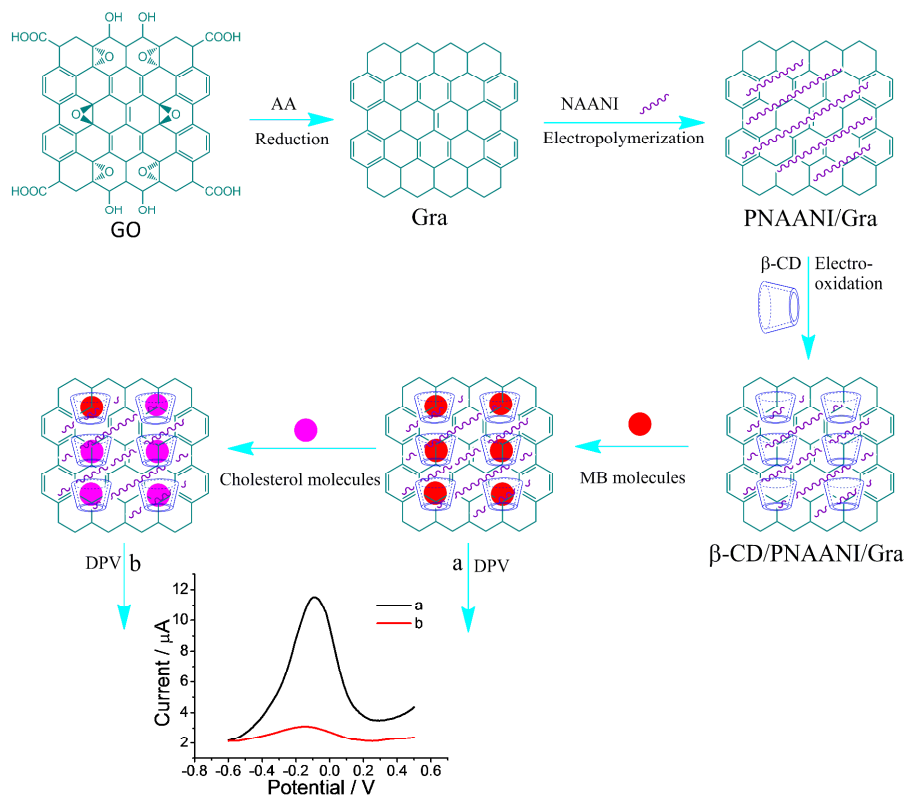
525

526

527

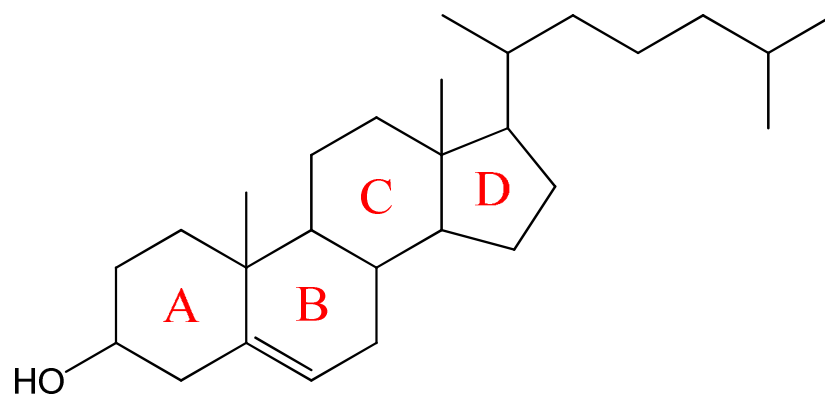
528

Figures:



Scheme 1.

Yang et al.



Scheme 2.

Yang et al.

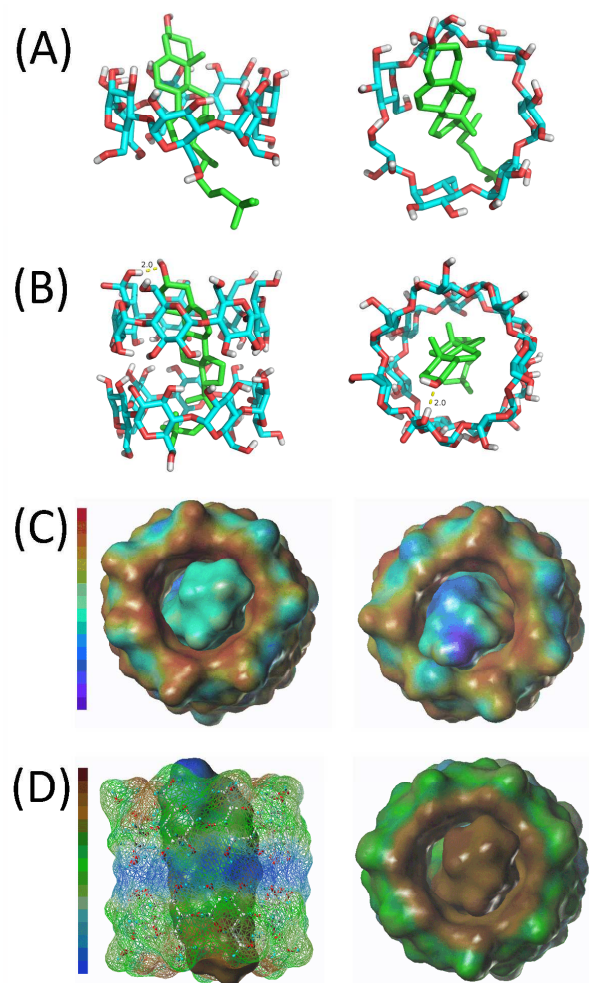
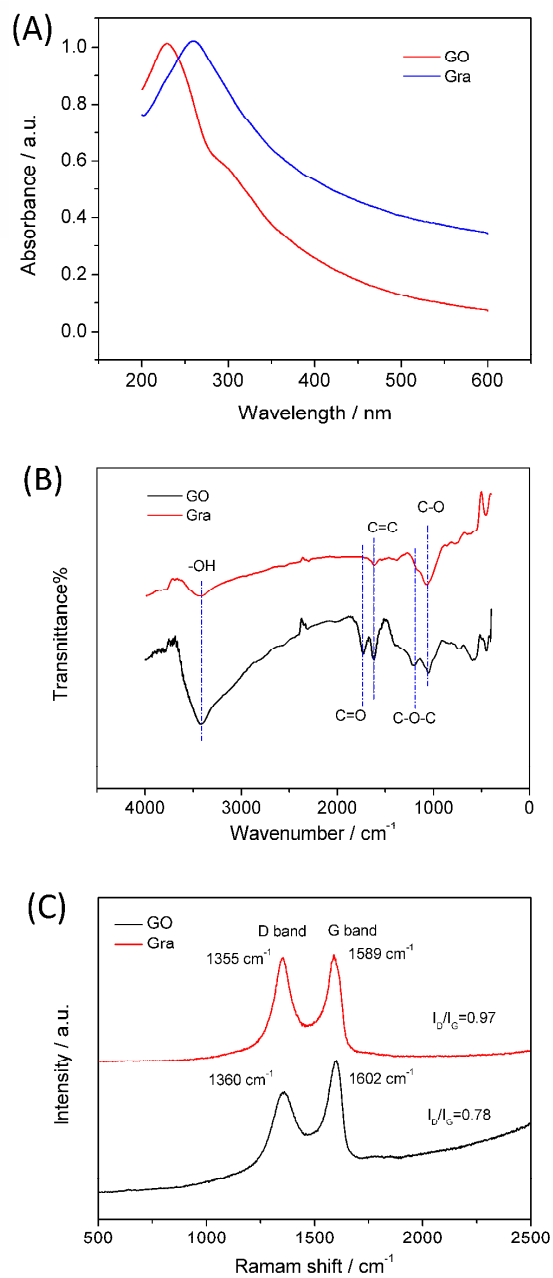


Fig. 1.

Yang et al.

**Fig. 2.****Yang et al.**

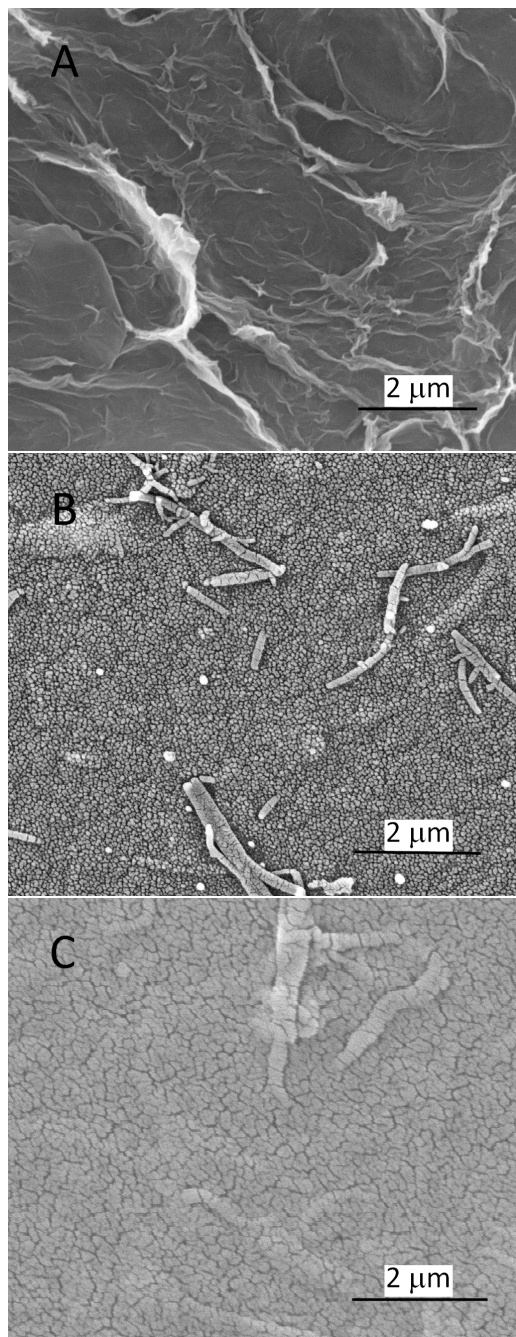
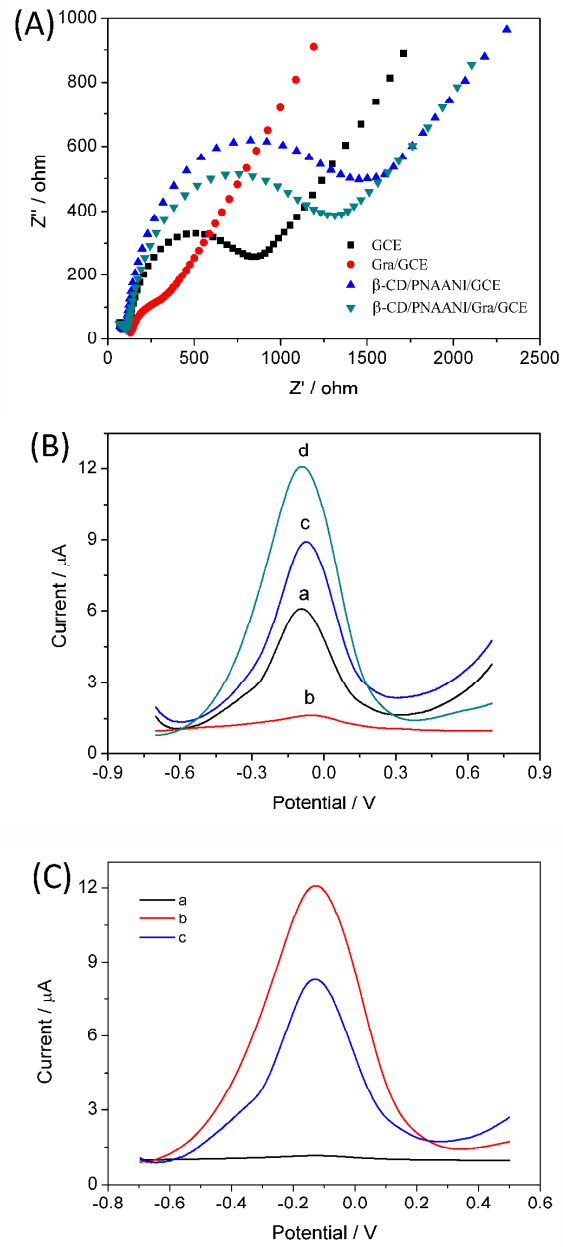
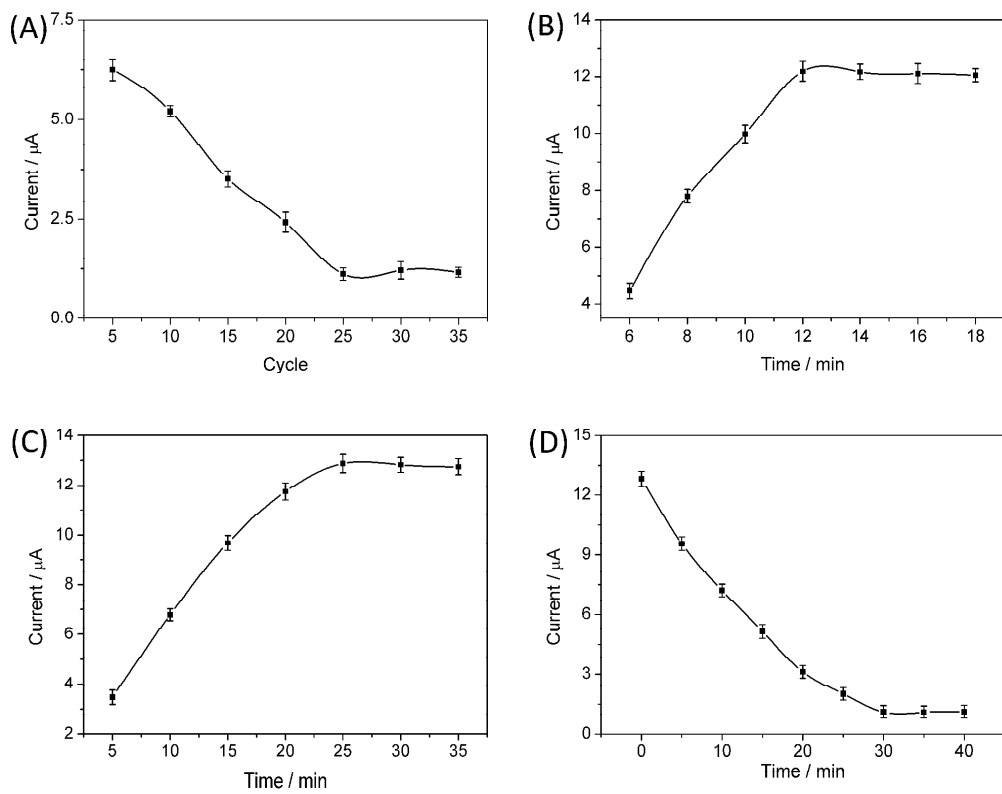
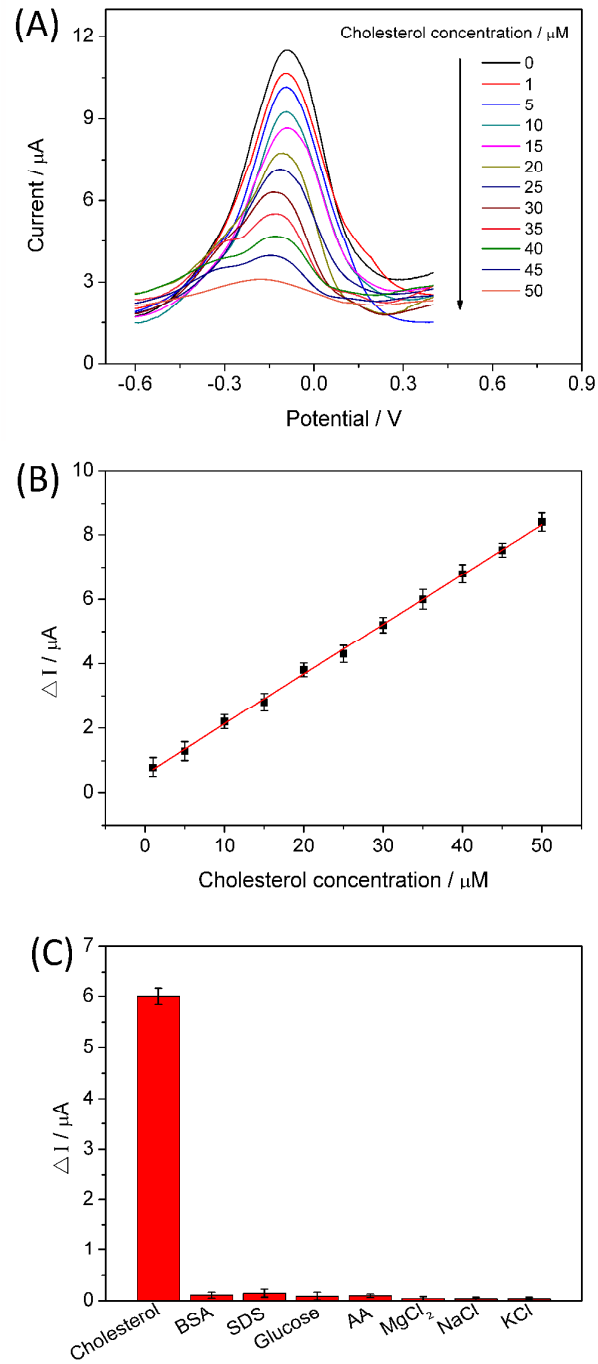


Fig. 3.

Yang et al.

**Fig. 4.****Yang et al.**

**Fig. 5.****Yang et al.**

**Fig. 6.**

Yang et al.

Table 1

The interaction energy between cholesterol and β -CD for 1:1 stoichiometry calculated by PM3 method.

System	Cluster rank	Number in cluster	ΔE (kcal/mol)
Cholesterol/ β -CD	1	23	-6.68
	2	7	-6.45
	3	8	-6.45
	4	4	-6.39
	5	2	-6.32
	6	1	-6.32
	7	2	-6.25
	8	2	-6.24
	9	1	-5.71

Table 2

Comparison of the present work with other recent literatures, using various electrode or matrix for cholesterol sensing.

Electrode or Matrix	Method	Liner range (μ M)	LOD (μ M)	Ref
Nafion/ChOx/GNPs-MWCNTs/GCE	DPV	10.0–5000.0	4.3	19
Chit-Hb/Chit-ChOx	amperometry	10.0–600.0	9.5	20
ChEt-ChOx/ZnO-CuO/ITO/glass	CV	500.0–12000.0	500.0	1
ChOx/PANI/PVP/Graphene	amperometry	50.0–10000.0	1.0	21
ChOx/Nano-ZnO/ITO	CV	130.0-10360.0	13.0	22
ChOx/ZnO(T)/CT/GCE	CV	400.0–4000.0	200.0	23
Nafion/ChOx/-Fe ₂ O ₃ /Ag	CV	100.0–8000.0	18.0	24
AuE/dithiol/AuNPs/MUA/ChOx	CV	40.0–220.0	34.6	5
Grp/ β -CD/Methylene Blue	DPV	1.0–100.0	1.0	17
Grp/ β -CD/Rhodamine 6G	Fluorescence	5.0–30.0	5.0	3
β -CD/PNAANI/Gra/GCE	DPV	1.0–50.0	0.50	This work

Table 3

Determination of cholesterol in human serum samples ($n=3$).

Sample	Added (μ M)	Founded (μ M)	RSD (%)	Recovery (%)
1	5.0	4.92 \pm 0.22	4.47	98.4
2	10.0	10.15 \pm 0.35	3.45	101.5
3	20.0	21.03 \pm 0.54	2.59	105.2

Tables

Yang et al.